AFM Characterization of Nanoscale Ribbons Grown from a Series of Oligo(p -phenyleneethynylene) Derivatives

ARTICLE *in* LANGMUIR · MARCH 2004

Impact Factor: 4.46 · DOI: 10.1021/la035505s · Source: PubMed

5 AUTHORS, INCLUDING:

Chuanzhen Zhou
North Carolina State University
25 PUBLICATIONS **305** CITATIONS
SEE PROFILE

Tai-Shung Chung
National University of Singapore
726 PUBLICATIONS **19,494** CITATIONS
SEE PROFILE

Zhi-Kuan Chen
Agency for Science, Technology and Researc…
89 PUBLICATIONS **2,715** CITATIONS
SEE PROFILE

AFM Characterization of Nanoscale Ribbons Grown from a Series of Oligo(*p*-phenyleneethynylene) Derivatives

Jingmei Xu,† Chuan-Zhen Zhou,† Lim Hup Yang,‡ Neal T. S. Chung,‡ and Zhi-Kuan Chen*,†

Institute of Materials Research & Engineering, 3 Research Link, Singapore 117602, and Department of Chemical & Environmental Engineering, National University of Singapore, 4 Engineering Drive 4, Singapore 117576

Received August 16, 2003. In Final Form: November 21, 2003

The key to optimizing the properties of molecular scale wires lies in understanding and controlling the solid-state morphologies. This paper examines the influence of oligomer chain length, solvent, and concentration on the formation of nanoscale ribbons on mica substrates from solutions of oligo(*p*-phenyleneethynylene)s (OPEs) with hexyloxy side chains and thioacetyl end groups. The OPEs are of different molecular chain lengths, in which the numbers of *p*-dihexyloxyphenyleneethynylene repeat units, *n*, are 1, 3, 5, and 7, respectively, with their two ends capped with 4-thioacetylphenyl alligator groups. The atomic force microscope (AFM) is employed to investigate the thin film morphology and study the self-assembled organizations. Solvent and concentration are found to exert a strong influence on thin film morphology. Under suitable conditions, OPEs with 7 *p*-dihexyloxyphenyleneethynylene repeat units are driven to form micrometer-long nanoribbons, oriented preferably along the 3-fold symmetry axes of the mica substrate. The cross section of the nanoribbons is composed of 7 molecules as evaluated by AFM characterization. On the other hand, oligomers with shorter chain lengths ($n = 1$, 3, and 5) produce thin films featuring globular nanoaggregates, chains consisting of elongated grains, and rods, respectively. Plausible reasons for the variation in thin film morphology are discussed, based on the results obtained from investigation of oligomer chain length, solvent, and concentration effects. A subtle balance among molecular size and physicochemical properties of solute molecules, solvent molecules, and substrate is crucial for the formation of desired structures. Among them, oligomer chain length plays a key role in thin film morphology, and the critical number of repeat units in OPE/poly(*p*-phenyleneethynylene) molecules for the formation of nanoribbon structures with a molecular cross section is supposed to be 8 or 9.

1. Introduction

Conjugated macromolecular materials have attracted increasing interest because they can be widely used as the active layers in optoelectronic devices such as solar cells,[1] light-emitting diodes (LEDs),[2] and field-effect transistors (FETs).[3] Their physical properties depend not only on the intrinsic single molecular characteristics but also on the supramolecular organization of the films.[4] The nature of the molecule, functionality, substrate, and thin film growth technique influence thin film properties.[5] Preparation of organic thin films with well-defined structural features is therefore crucial both for fundamental research and for realization of optimal molecular devices. Well-defined π-conjugated oligomers can play an important role in this field because their precise chemical structure and conjugation length lead to defined functionality and facilitate control over their supramolecular structures.[6]

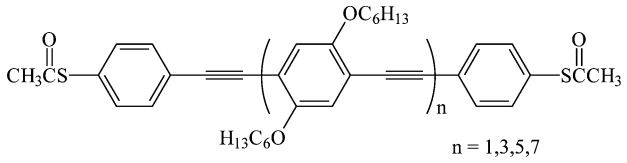

OPE-SAc-n, n = 1, 3, 5, 7

Figure 1. Chemical structure of the OPE-SAc-*n* oligomers.

In this paper, we report the growth and atomic force microscope (AFM) characterization of self-assembled supramolecular organizations from a series of functionalized oligo(*p*-2,5-dihexyloxyphenyleneethynylene) derivatives (OPEs) with thioacetyl (SAc) end groups. The chemical structures of the OPEs are shown in Figure 1.

Details of their synthesis have been reported previously.[7] The numbers of repeat units (*n*) of the *p*-dihexyloxyphenyleneethynylene moiety in the SAc-capped OPEs are 1, 3, 5, and 7, respectively. The OPEs with SAc end groups employed in this work are therefore denoted as OPE-SAc-*n* (n =1, 3, 5, 7), respectively, as shown in Figure 1.

The thioacetyl groups at the ends of OPEs chains can be deprotected and facilitate chemical attachments with gold nanoelectrodes. Conjugated backbones based on *p*-phenyleneethynylene repeat units have been chosen because of their stiffness,[8] good solubility after function-

* Corresponding author. E-mail: zk-chen@imre.a-star.edu.sg. Fax: (65) 6872 0785.
† Institute of Materials Research & Engineering.
‡ National University of Singapore.

(1) Yu, G.; Gao, J.; Hummelen, J. C.; Wudl, F.; Heeger, A. J. *Science* **1995**, *270*, 1789.
(2) Bourroughes, J. H.; Bradley, D. D. C.; Brown, A. R.; Marks, R. N.; MacKay, K.; Friend, R. H.; Burn, P. L.; Holmes, A. B. *Nature* **1990**, *347*, 539.
(3) Sirringhaus, H.; Tessler, N.; Friend, R. H. *Science* **1998**, *280*, 1741.
(4) Ziegler, C. In *Handbook of Organic Conductive Molecules and Polymers*; Nalwa, H. S., Eds.; Wiley: Chichester, U.K., 1997; Vol. 3, Chapter 13.
(5) Bäuerle, P.; Fischer, T.; Bidlingmeier, B.; Stabel, A.; Rabe, J. P. *Angew. Chem., Int. Ed. Engl.* **1995**, *34*, 303.
(6) Martin, R. E.; Diederich, F. *Angew. Chem., Int. Ed.* **1999**, *38*, 1350.
(7) Zhou, C. Z.; Liu, T. X.; Xu, J. M.; Chen, Z. K. *Macromolecules* **2003**, *36*, 1457.

10.1021/la035505s CCC: $27.50
Published on Web 01/06/2004

alization with pendant chains,[9] high and stable photoluminescence quantum yield,[10] and relatively low defect density along the conjugated backbone.[11] Samorí et al. have investigated the supramolecular structures of poly(*p*-phenyleneethynylene) derivatives (PPEs) with repeat unit numbers of the *p*-dihexylphenyleneethynylene moiety more than 9 and successfully driven the PPE self-assembly into micrometer-long nanoribbons with a molecular cross section.[12−15] They proposed a model architecture to explain the supramolecular structure of the self-assembled nanoribbons, in which a ribbon is composed of parallel and fully extended backbones stacked perpendicular to the main ribbon axis in a bilayer/trilayer aggregate with the side chains perpendicular to the substrate.[13−15] Their results showed that PPEs with repeat units from 9 to 22 were driven toward the formation of nanowires but those with more repeat units were not. This information seems to suggest that a suitable molecular chain length is required for the formation of nanowires. In the current report, we examine the thin films of OPEs with repeat unit numbers going from 1 to 7 and end functional groups of SAc. It is found that the number of repeat units exerts key influence on the formation of nanostructures. Solvent and concentration are also found to play important roles in thin film morphology. Possible reasons for the observations are discussed.

2. Experimental Section

Materials. The synthesis of OPEs has been reported previously.[7] As-received tetrahydrofuran (THF) (AR, TEDIA), toluene (AR, Merck), and *n*-octylbenzene (>98%, TCI) were used as solvents or components in mixture solvents for the preparation of oligomer solutions. Before evaporative casting, all the solutions were filtered through poly(tetrafluoroethylene) (PTFE) filter devices with 0.2 μm pore size. Muscovite mica of grade V-4 was obtained from SPI Supplies, West Chester, PA, and cleaved freshly prior to use.

Thin Film Preparation. Solutions with different concentrations (0.2−0.3 to 0.01−0.15 mg/mL) of OPEs in THF, toluene, or THF/*n*-octylbenzene 5:1 and THF/*n*-octylbenzene 2.5:1 mixtures were prepared and filtered. Molecular self-assembly was accomplished by applying one drop of solution onto a freshly cleaved mica surface and allowing the solvent to evaporate in air at room temperature. The mica plates were covered with 50 mL beakers to protect the mica surfaces from dust. This may also help create a relatively confined space and make the evaporation of solvents slower as compared to that in an open-air environment. At least two thin films were prepared for one sample. Tens of AFM scans were made for each thin film, and the images from different thin films showed that the morphological reproducibility is good for one specific sample.

Atomic Force Microscope. Investigation of the surface morphology of the OPE thin films was conducted in contact mode on a ThermoMicroscope Autoprobe CP Research AFM system, from Park Scientific Instrument, Sunnyvale, CA. Conical silicon nitride terminal tips mounted on silicon cantilevers with a force constant of 0.26 or 0.40 N/m were employed. The manufacturer specification for the terminal tip radius of curvature is on average 10 nm (5−30 nm). The silicon cantilevers have a length of 180 μm, width of 25 or 38 μm, thickness of 1 μm, and resonant frequency of 40 or 45 kHz. All the images reported were topographies and were simply processed by flattening and sometimes deglitching, using IP2.1 image software provided by the manufacturer.

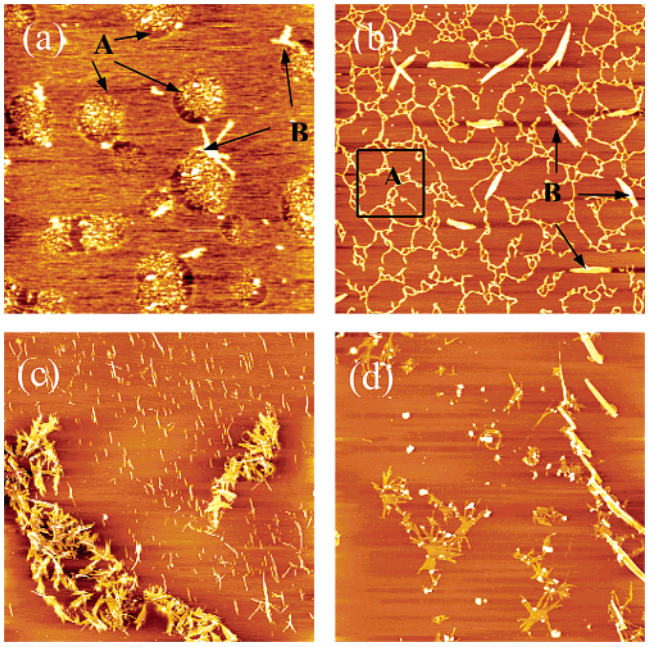

Figure 2. AFM images of OPE-SAc-7 on mica cast from four solvents: (a) THF, scan size 10 × 10 μm, height range from region measurement (peak−valley) h = 44.62 nm; (b) toluene, scan size 10 × 10 μm, h = 34.72 nm; (c) THF/*n*-octylbenzene 5:1, scan size 30 × 30 μm, h = 30.71 nm; (d) THF/*n*-octylbenzene 2.5:1, scan size 30 × 30 μm, h = 95.88 nm.

Contact Angle Measurement. Oligomer thin films for contact angle measurement were spin cast from chloroform solution. Advancing and receding contact angles of glycerol on the thin films were measured on a Ramé-Hart contact angle goniometer equipped with a tilting base.[16]

3. Results and Discussion

Influence of Solvent. It was reported that solvents used to prepare thin films exerted a strong influence on the thin film morphology and the structure of the supramolecular organization of PPEs, due to the differences in volatility.[14] We examined the influence of different solvents on thin film morphology in order to choose a suitable solvent for the preparation of the desired nanoribbon structure. Employing OPE-SAc-7 as the thin film forming material, we examined the following four types of solvents: THF (bp, 67 °C); toluene (bp, 110 °C); a mixture of THF and *n*-octylbenzene (5:1) (bp of *n*-octylbenzene, 262 °C); a mixture of THF and *n*-octylbenzene (2.5:1).

Figure 2a−d shows the AFM topographical images representing the morphologies of the OPE-SAc-7 thin films cast on mica surfaces from THF, toluene, and THF/*n*-octylbenzene 5:1 and THF/*n*-octylbenzene 2.5:1 mixture solutions at a concentration of 0.2−0.3 mg/mL. The image of the thin film from THF (Figure 2a) shows an irregular distribution of patches mostly round in shape. Two types of patches were observed. Some are disklike, and some are part-ring−part-disk-like (indicated by arrows A). Sometimes there are also rodlike or irregularly shaped aggregates lying beside or above the patches, as indicated by arrows B.

(8) Moroni, M.; Le Moigne, J.; Luzzati, S. *Macromolecules* **1994**, *27*, 562.
(9) Ofer, D.; Swager, T. M.; Wrighton, M. S. *Chem. Mater.* **1995**, *7*, 418.
(10) Weder, C.; Wrighton, M. S. *Macromolecules* **1996**, *29*, 5157.
(11) Egbe, D. A. M.; Roll, C. P.; Klemm, E. *Des. Monomers Polym.* **2002**, *5*, 245.
(12) Samorí, P.; Francke, V.; Mangel, T.; Müllen, K.; Rabe, J. P. *Opt. Mater.* **1998**, *9*, 390.
(13) Samorí, P.; Francke, V.; Müllen, K.; Rabe, J. P. *Thin Solid Films* **1998**, *336*, 13−15.
(14) Samorí, P.; Francke, V.; Müllen, K.; Rabe, J. P. *Chem.—Eur. J.* **1999**, *5*, 2312.
(15) Samorí, P.; Sikharulidze, I.; Francke, V.; Müllen, K.; Rabe, J. P. *Nanotechnology* **1999**, *10*, 77.
(16) Extrand, C. W.; Kumagai, Y. *J. Colloid Interface Sci.* **1996**, *184*, 191.

The morphology of the OPE-SAc-7 thin film cast from 0.2−0.3 mg/mL toluene solution is typically shown in Figure 2b. It consisted of two types of aggregates: network structures and rodlike aggregates, as indicated by frame A and arrows B, respectively. The whole thin film surface was dominated by a network structure but decorated with rodlike aggregates. In addition to these typical structures, there was no patchy morphology observed in tens of scans.

The representative morphologies of the thin films prepared from THF/*n*-octylbenzene 5:1 and THF/*n*-octylbenzene 2.5:1 mixture solutions are displayed in panels c and d of Figure 2, respectively. Irregular aggregates consisting of random needles were observed in the thin film cast from the former solution (the lower left part of Figure 2c). Nanoribbons were also found beside the irregular aggregates in some areas of the thin film. The nanoribbons aligned with reference to each other at an angle of about 60°. The thin film morphology of OPE-SAc-7 cast from THF/*n*-octylbenzene 2.5:1 mixture solvent was dominated by irregular aggregates consisting of random crystalline needles, as shown in the left part of Figure 2d. However, very scarcely, rods, which are bigger in height, length, and width, were observed as shown in the right part of Figure 2d. Both the needles and rods did not show an obvious orientation on the mica surface.

From the above observation, we can see that the morphology and structure of the OPE-SAc-*n* thin films change with solvent. With the decrease in volatility from THF to toluene, the self-assembly of OPE-SAc-7 thin films cast from toluene was driven toward a more ordered direction as compared to that from THF, as shown in panels b and a of Figure 2, respectively. When the solvent was changed to the THF/*n*-octylbenzene 5:1 mixture (Figure 2c), some areas of the thin film were found to grow nanoribbons with orientation, but most of the areas were aggregates composed of random crystalline needles. However, when the ratio of *n*-octylbenzene to THF was further increased to 1:2.5, the morphology of the thin films was dominated by irregular aggregates composed of random needles as shown in the left part of Figure 2d. Even the very scarcely observed rods (in the left part of Figure 2d) did not show obvious orientation. This implies that a solvent with too high or too low a volatility is unfavorable for the nanoribbon formation.

Samorí et al. indicated that the molecular organization on the mica substrate is attributed to the solvent evaporation process that is followed by the self-assembly of the organic compound into the ribbon structure.[13] They proposed that the ribbon formation process might be divided into two steps: aggregation of the molecules into straight ribbons and self-assembly of the oriented ribbons induced by the underlying crystalline substrate. On the basis of the different morphologies shown in Figure 2, we think that, similar to that reported by Samorí et al., the nanoribbon formation is governed by the above two processes, and the two processes take place not one by one but simultaneously. The latter hypothesis is supported by the result that the crystalline needles or rods did not orient according to the mica symmetry axes although rods and needles were formed when THF/*n*-octylbenzene 2.5:1 was used as the solvent.

The morphological difference in the thin films cast from THF, toluene, and THF/*n*-octylbenzene 5:1 and THF/*n*-octylbenzene 2.5:1 solutions, as shown in Figure 2, also suggests that the self-assembly and aligning process is a result of many kinds of interactions, in addition to the influence of solvent volatility. These may include the interactions between the conjugated macromolecules, between the solvent molecule and solute molecule, and between the underlying substrate and the solute and solvent molecules. The collective effect of these interactions and a subtle balance among them lead to the formation and alignment of ordered structures. Other researchers also reported similar effects and emphasized that the subtle balance among hydrophilicity and hydrophobicity of the substrate surface, solvent and solute molecules, and structure and shape of the solute molecule controlled the ordered alignment.[17,18] In the current work, THF is hydrophilic while toluene and *n*-octylbenzene are hydrophobic. Therefore, the hydrophilicity of the four solvents is in the order THF > THF/*n*-octylbenzene 5:1 > THF/*n*-octylbenzene 2.5:1 > toluene. This suggests that THF is the most spreadable solvent and has the strongest wetting ability on the mica surface among them. On the other hand, the low boiling point of THF leads to fast evaporation. We speculate that the fast evaporation as well as the good wetting property of THF give rise to the formation of disklike and half-ring−half-disk patchy structures.

Ring and disk structures have been observed in thin films of organosiloxane derived from $SiCl_3$-terminated dendrons.[19] It was explained that the liquid flow drags solute toward the rim of a hole and/or a droplet and pins the contact line, which defines the ring or disk after the solvent dries out. The formation of droplets or holes in an evaporating film is primarily driven by the instability of the film when it thins to a critical thickness, as indicated by both theoretical and experimental studies.[20,21] Beyond this thickness, nucleation (homogeneous nucleation from surface undulation and heterogeneous nucleation from impurities in the thin film or on the substrate[22] or from defects on the substrate) can rupture the film to form holes usually with a circular shape to minimize surface energy. Continuously thinning the film by evaporation expands the holes. If the rims of the holes cannot be pinned by the solute, they will "percolate" to form droplets at their interstices.[23] This applies to both dewetting and wetting substrates, of which the latter is related to one of our systems with pure THF as the solvent.[24] We think that droplets formed at the late stage of solvent evaporation, leading to the formation of disklike and half-ring−half-disk patches. On the other hand, although THF evaporates fast, some molecules may happen to come together and aggregate in a more ordered structure to form a rodlike structure (indicated by arrows B in Figure 2a). This is because the OPEs have a very rigid structure and there is strong intermolecular interaction among them.

When toluene was employed as the solvent, the interaction between the hydrophobic toluene solvent and the hydrophilic mica substrate led to dewetting of the solvent on the substrate, instead of wetting. The dewetting of toluene and the not very strong interfacial interaction between OPE-SAc-7 and the mica surface may be responsible for the lack of patchy morphology in Figure 2b.

(17) Hellmann, J.; Hamano, M.; Karthaus, O.; Ijiro, K.; Shimomura, M.; Irie, M. *Jpn. J. Appl. Phys.* **1998**, *37*, L816.
(18) Li, J.; Qin, D. J.; Baker, J. R., Jr.; Tomalia, D. A. *Macromol. Symp.* **2001**, *166*, 257.
(19) Xiao, Z. D.; Cai, C. Z.; Mayeux, A.; Milenkovic, A. *Langmuir* **2002**, *18*, 7728.
(20) Sharma, A.; Khanna, R. *J. Chem. Phys.* **1999**, *110*, 4929.
(21) Oron, A.; Davis, S. H.; Bankoff, S. G. *Rev. Mod. Phys.* **1997**, *69*, 931.
(22) Gu, X.; Raghavan, D.; Douglas, J. F.; Karim, A. *J. Polym. Sci., Part B: Polym. Phys.* **2002**, *40*, 2825.
(23) Ohara, P. C.; Gelbart, W. M. *Langmuir* **1998**, *14*, 3418.
(24) Padmakar, A. S.; Kargupta, K.; Sharma, A. *J. Chem. Phys.* **1999**, *110*, 1735.

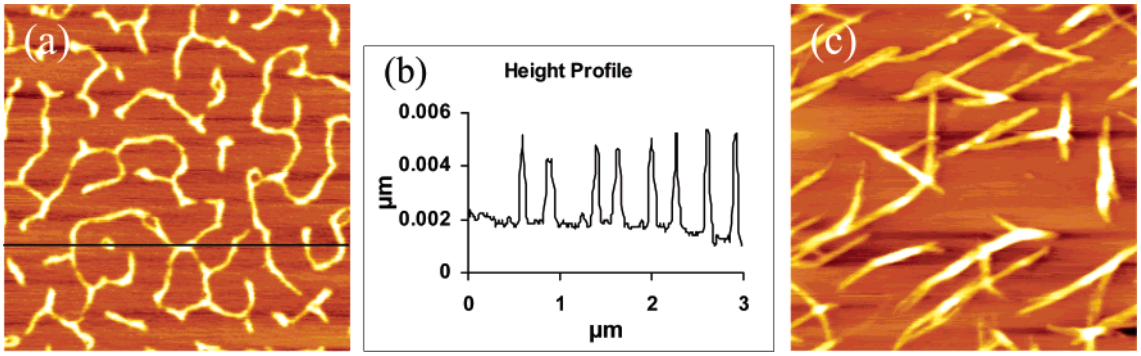

Figure 3. (a) AFM images of OPE-SAc-7 on mica cast from toluene, scan size 3 × 3 μm, h = 7.04 nm; (b) topographical profile along the black line indicated in Figure 2a; (c) AFM images of OPE-SAc-7 obtained from the same sample as in Figure 2a but a different area, scan size 10 × 10 μm, h = 24.06 nm.

From another point of view, toluene has a higher boiling point and evaporates slower than THF. The moderate volatility and dewetting of toluene bring the OPE-SAc-7 molecules together, and they aggregate as rodlike and network structures.

When the solvent was changed from THF or toluene to THF/*n*-octylbenzene (5:1), the evaporation was slowed. The strong intermolecular interaction between OPE-SAc-7 molecules and the significantly slowed evaporation rate of the solvent provide OPE-SAc-7 molecules with enough time to get together and self-assemble into crystalline organizations. However, as will be discussed later, the current concentration (0.2−0.3 mg/mL) is too high and hence, some areas of the mica surface accumulate too many OPE-SAc-7 molecules. Hence, although the OPE-SAc-7 molecules self-assemble into crystalline organizations, most of them have insufficient room to align according to the 3-fold symmetry axes of the mica substrate during the self-assembly process. As a result, randomly distributed crystalline aggregates dominated the image, as shown in the lower left part of Figure 2c. Beside the random crystalline aggregates, some areas were occupied by orientated nanoribbons, aggregated from the local solution of relatively low concentration. The accumulation of OPE-SAc-7 molecules with different densities at the mica surface and hence the formation of ordered nanoribbons and random crystalline aggregates may be considered as the result of thin film rupture, when the thinning of the film reaches a critical thickness, as discussed above.

When the *n*-octylbenzene content in the solvent was increased further to THF/*n*-octylbenzene 2.5:1, an adverse effect resulted. As shown in Figure 2d, although the thin film is made of crystalline needles and rods, they are not aligned along any obvious direction. We hypothesize that, in addition to decreasing the volatility of the solvent, more *n*-octylbenzene content also brings the solvent higher viscosity, lower wettability, and a stronger interaction between OPE-SAc-7 and solvent molecules (mainly between OPE-SAc-7 and *n*-octylbenzene). Consequently, the interaction between the OPE-SAc-7 molecule (or its self-assembly) and the mica surface was reduced, resulting in no domination in orientation of the self-assembled organizations.

In view of the above results, an optimum evaporation rate and a balance among hydrophilicity and hydrophobicity and other physicochemical properties of the solute and solvent molecules as well as of the mica surface have to be reached, to facilitate the formation of oriented nanoribbons. Throughout the experiments, the THF/*n*-octylbenzene 5:1 mixture seems to provide the best condition for the self-assembly of the OPEs on the mica surface.

Influence of Concentration. The concentration of the solutions used in thin film formation influences the morphology greatly.[12] Our studies on solvent influence also revealed that thin film morphological variations sometimes were induced by local concentration differences, as shown in Figure 2c. To find a suitable concentration range for the nanoribbon formation, we roughly examined the concentration effect on thin film morphology.

The image in Figure 2b was dominated by network and rod structures at a concentration of 0.2−0.3 mg/mL. When the concentration of the toluene solution was reduced by half (0.1−0.15 mg/mL), the thin film morphology changed to a mazelike structure with oriented nanoribbons found at some areas. The two types of morphologies are shown in panels a and c of Figure 3, respectively. The mazelike structure is made of connected and randomly aligned nanoscale lines, with an apparent width of 58−80 nm and height of 2.3−3.1 nm. The lateral broadening effect due to the tip shape as calculated similarly to the way used by Samorí et al.[12] is about 6.3−7.2 nm. Therefore, the actual line width of the network structure is about 50−73 nm after subtracting the tip broadening effect. As the contour length of the OPE-SAc-7 molecule is 6.65 nm (calculated using the values reported in the literature[12−15]), the cross section of the lines composing the mazelike structure is not molecular but multimolecular, if the self-assembly structure of OPE-SAc-7 is similar to the one proposed by Samorí et al.[13−15] It is not surprising that the structural feature in Figure 3a is similar to the network structure shown in Figure 2b because the concentration does not differ drastically in the two cases. The formation of the mazelike structure is similarly attributed to the dewetting property of toluene on the mica surface as well as its moderate evaporation. However, in some areas of the thin film, nanoribbon structures with preferable orientation as shown in Figure 3c were observed. The width and height of the ribbons are 160−330 nm and 4.8−13 nm, respectively. The nanoribbons align with reference to each other at roughly an angle of 60°, indicating a pseudoepitaxial growth according to the 3-fold symmetry axes of the mica surface. The nanoribbon structure was only found very scarcely, and the formation of the nanoribbons from toluene solution may be attributed to the relatively late drying out of the thin film because of locally "slow" evaporation of toluene in some area, which is "lower" in height and thus has more toluene accumulation due to the existence of, for example, steps. It can be concluded that thin film structures depend to a large extent on the local kinetics of solvent evaporation in addition to concentration and solvent effects, and different structures are formed when the kinetics are not equivalent over the whole sample.

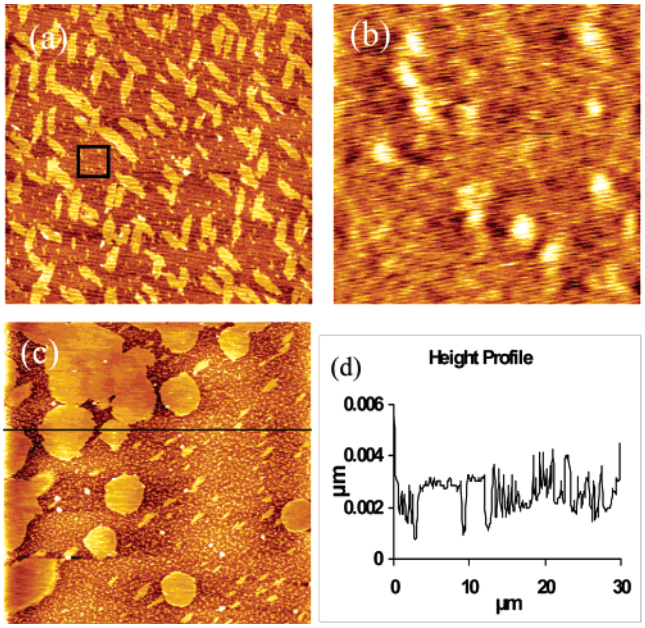

Figure 4. (a) AFM images of OPE-SAc-1 on mica cast from THF/*n*-octylbenzene 5:1. Scan size 10 × 10 μm, h = 12.16 nm. (b) Enlarged AFM image of the area indicated by the black square in panel a. Scan size 1 × 1 μm, h = 2.38 nm. (c) AFM images of OPE-SAc-3 on mica cast from THF/*n*-octylbenzene 5:1. Scan size 30 × 30 μm, h = 25.19 nm. (d) Topographical profile along the black line indicated in panel c.

Although an ordered nanoribbon structure was observed in thin films prepared from a toluene solution of suitable concentration, we do not think toluene is a good solvent for nanoribbon formation. This is because nanoribbons were a very rare occurrence in the thin film and the width of the nanoribbons is big and the height of the nanoribbons varies greatly. On the basis of the results summarized from Figures 2 and 3, the solvent suitable for the nanoribbon growth seems to be THF/*n*-octylbenzene 5:1, as mentioned above. Thin film morphologies of OPE-SAc-*n* (n = 1, 3, 5, 7) prepared from different concentrations were investigated using the AFM. It was found that OPE-SAc-*n* (n =1, 3, 5) thin films exhibit similar structural features at relatively high (0.2−0.3 mg/mL) concentration, that is, leaflike and/or circular patches. Panels a and c of Figure 4 display the images at 10 × 10 μm scan size for OPE-SAc-1 and OPE-SAc-3, respectively. The image for OPE-SAc-5 was not shown because of the similarity in its structural feature: leaflike islands but aligned along one direction only. The OPE-SAc-1 thin film consisted of leaflike islands. They align along mainly two directions at an angle of about 60° and have a height of 0.95 ± 0.23 nm. One area beside the leaflike islands as indicated by the black square in Figure 4a was enlarged at a 1 × 1 μm scan size, and the image is shown in Figure 4b. It can be seen that the area beside the leaflike islands is not blank but covered by nanoaggregates. In Figure 4c, the thin film morphology of OPE-SAc-3 displays leaflike islands and roughly round patches. The topographical profile along the line indicated in Figure 4c is shown in Figure 4d. It can be seen that the uppermost surfaces of the patches are almost flat and the height is about 2 nm, corresponding to a single molecular layer if the molecules stand with the side chains perpendicular and backbones parallel to the substrate, because the width of the molecule with the hexyloxy side chains extended is 2.0 nm (calculated according to literature values[12−15]). In addition to the two features, the rest of the thin film is covered by nanoaggregates and their heights are less than or equal to those of the islands and patches. The nanoaggregates may be formed in a locally less concentrated solution, and the molecules inside the aggregates may not stand straight on the surface in a single layer. This situation happens more with oligomers with fewer repeat units, such as OPE-SAc-1 and OPE-SAc-3. This may be because the two molecules have a relatively higher content of SAc end groups and thus stronger dipole−dipole interaction at the ends of the oligomers and weaker $\pi-\pi$ interaction between the oligomer backbone, leading to the development of leaflike islands, which are shorter and wider and more irregular in shape as compared to nanoribbons or rods. The OPE-SAc-7 thin film displays no leaflike structure (Figure 2c) but random crystalline aggregates and oriented nanoribbons, possibly due to the stronger interaction between oligomer backbones and weaker dipole−dipole interaction between the ends of OPE-SAc-7 molecules.

To obtain some experimental information relating to the physicochemical properties of the OPEs, we have measured the contact angles of glycerol on OPE thin films. The glycerol contact angles on OPE-SAc-*n* thin films are 77.5 ± 0.6, 80.0 ± 0.5, 83.0 ± 0.4, and 85.7 ± 0.4° for n = 1, 3, 5, and 7, respectively. The result indicates that the hydrophilicity of the OPEs decreases with the increase of oligomer chain length. This is in accordance with the decreased dipole−dipole interaction between the SAc groups, decreased interaction between the OPEs and the mica substrate, and therefore increased interaction between OPE backbones with the increase of OPE chain length.

In summary, the concentration of 0.2−0.3 mg/mL favors the formation of leaflike islands, patches, or random crystalline aggregates. A lower concentration at about 0.1−0.15 mg/mL is suitable for the potential growth of nanoribbons with ordered alignment, as will be discussed in the next section.

Thin Films of OPE-SAc-*n*: Influence of the Number of Repeat Units and Formation of Nanoribbons. The results obtained from the previous sections indicate that employing THF/*n*-octylbenzene 5:1 as the solvent and preparing the thin films with solutions at a concentration of about 0.1−0.15 mg/mL are likely to yield nanoribbons. Panels a and b of Figure 5 display the AFM topographical images of thin films prepared under the chosen conditions for OPE-SAc-1 and OPE-SAc-3, respectively. Randomly distributed globular nanoaggregates similar to those found beside leaflike islands in the previous section were observed dominating the OPE-SAc-1 thin films (Figure 5a). For the thin films of OPE-SAc-3, the morphology is mainly composed of not very straight linelike features with different heights, widths, and lengths and roughly aligning toward one direction. At higher magnification as shown in Figure 5c, it can be seen clearly that the "lines" are actually chains composed of loosely connected elongated grainy aggregates. The height of the chains in Figure 5b ranges from 1.0 to 5.4 nm, and the width from 50 to 138 nm.

The thin film morphologies of OPE-SAc-5 and OPE-SAc-7 are shown in panels a and b of Figure 6, respectively. The former molecules self-assemble into rods with differing lengths, widths, and heights. The length of the rod varies from 1.1 to 4.0 μm, and the width from 400 to 1100 nm, while the height is 4.01 ± 0.63 nm. When the oligomer chain length increases further from 5 to 7 repeat units, great morphological change was detected from AFM images, as shown in Figure 6b. Instead of rods, nanoribbons are the dominating thin film feature for OPE-SAc-7. The nanoribbons can be as long as a few micrometers, and there is no great variation in height

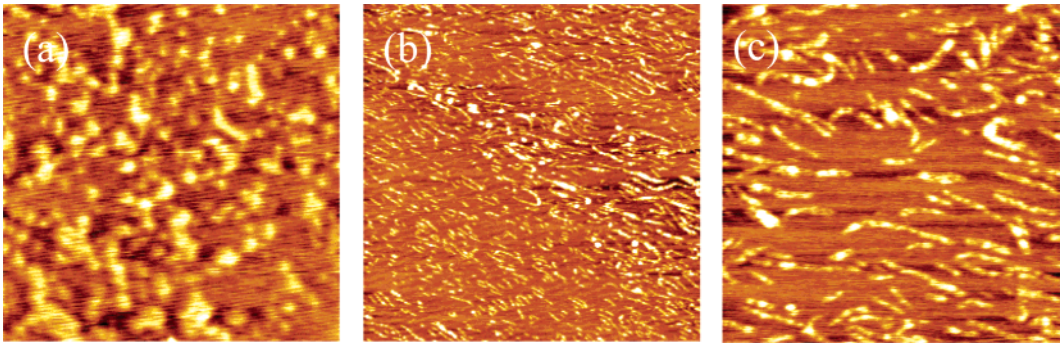

Figure 5. AFM images of OPE-SAc-*n* on mica cast from THF/*n*-octylbenzene 5:1 at a concentration of 0.1−0.15 mg/mL. (a) OPE-SAc-1, scan size 3 × 3 μm, h = 3.38 nm. (b) OPE-SAc-3, scan size 10 × 10 μm, h = 11.28 nm. (c) An enlarged image of OPE-SAc-3 (not from the image shown in panel b), scan size 3 × 3 μm, h = 7.75 nm.

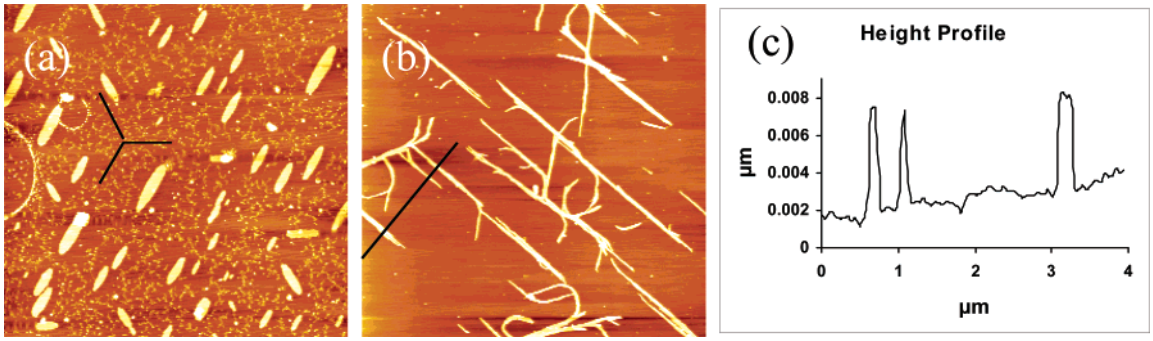

Figure 6. AFM images of OPE-SAc-*n* on mica cast from THF/*n*-octylbenzene 5:1 at a concentration of 0.1−0.15 mg/mL. (a) OPE-SAc-5, scan size 30 × 30 μm, h = 47.00 nm. The black lines serve as a guide for the 3-fold symmetry axes of the mica substrate. (b) OPE-SAc-7, scan size 10 × 10 μm, h = 30.71 nm. (c) Topographical profile along the black line indicated in panel b.

(4.27 ± 0.74 nm). The width of the ribbons varies from 42 to 130 nm after subtracting the tip broadening effect. The thicker ribbons seem to be formed by the aggregation of two, three, or even more "basic" ribbons. The topographical profile as indicated by the black line in Figure 6b is shown in Figure 6c, displaying three nanoribbons composed of two, one, and three basic ribbons, respectively. The cross section of the basic nanoribbons is 42 nm, corresponding to an aggregation of about 7 molecules considering the dipole−dipole interaction between the SAc end groups and thus the possible interdigitation among them, if the molecules lie parallel to each other with their molecular backbones perpendicular to the long axis of the ribbons. The height of the ribbon suggests a bilayer packing if the side chains are perpendicular to the substrate surface.

Because of the similarity of the molecular structures of OPE-SAc-*n* to those of the PPEs used by Samorí et al.[12−15] and the coincidence of the height of the nanoribbons to the doubled calculated molecular width of the OPE molecules, we tend to believe that the OPE-SAc-7 molecules self-assemble into the nanoribbon structures in a way very similar to that proposed by Samorí et al.: that is, the molecules lie parallel to each other with their backbone chains perpendicular to the ribbon long axis but the hexyloxy side chains perpendicular to the substrate surface. However, in their report, the cross section of nanoribbons was molecular, while in the current report, the cross section of the ribbons suggests an aggregation of 7 molecules in the width axes of the OPE-SAc-7 nanoribbons. This difference may be attributed to the differing oligomer/polymer chain length. The PPEs employed by Samorí et al. have at least 9 *p*-dihexylphenyleneethynylene repeat units, while OPE-SAc-7 studied in the current work has only 7 similar repeat units. The anisotropy in the former polymers is thus stronger than in the latter oligomer. The driving forces for the self-assembly of the OPE/PPE molecules into the ordered ribbon structure are the $\pi-\pi$ interaction between the OPE/PPE backbones, their strong stiffness and anisotropy, and the interfacial force between the solute molecules and the substrate. In the current report, the chain lengths of the oligomers are shortened as compared to those of PPEs; the interaction between the anisotropic OPEs backbones is decreased, while the dipole−dipole interaction between the SAc end groups in neighboring molecules is strengthened as compared to that in PPEs. This leads to a decreased tendency to form nanoribbons with molecular cross section. The trend that the width of the rod/nanoribbons decreases from OPE-SAc-5 to OPE-SAc-7 is in agreement with the explanation, but OPE-SAc-5 may also self-assemble into rods in a bilayer structure because their height is 4.01 ± 0.63 nm. As for oligomers with shorter chains, such as OPE-SAc-1 and OPE-SAc-3, it is not surprising that the nanoaggregates from the former are not anisotropic organizations, while the latter formed elongated grains and the grains tended to connect loosely with each other to form micrometer-long chains. In view of the results reported in this work and those in the literature,[12−15] the critical length for OPEs/PPEs with side chains to form nanoribbons with a molecular cross section is such that the number of *p*-phenyleneethynylene repeat units in the molecules is 8 or 9.

4. Conclusion

To grow nanoribbons from a series of OPEs with hexyloxy side chains and thioacetyl end groups, which will facilitate chemical attachment with gold nanoelectrodes and potentially be used in nanoelectronics, we have investigated the thin film morphologies prepared from these oligomers with different chain lengths. To find a suitable solvent for the nanoribbon growth, the solvent

influence on the morphology of the thin films cast from four solvents was examined. Reasons for the solvent effects were discussed, and the results indicated that the thin film morphology is influenced by many interactions including those between solute and solute molecules, between solute and solvent molecules, and between the substrate surface and the solute/solvent molecules. THF/*n*-octylbenzene 5:1 was found to be a good solvent for the nanoribbon formation from these oligomers. The concentration of the oligomer solutions also strongly influenced the thin film morphology, and a concentration of about 0.1−0.15 mg/mL was suitable for the formation and detection of thin film characterization. Thin films cast from oligomers with different repeat units were observed to display very different morphologies, in which globular aggregates, chains composed of elongated grains, rods, and nanoribbons with a cross section consisting of about 7 molecules were found for the OPEs with 1, 3, 5, and 7 repeat units, respectively. The critical number of repeat units for the formation of nanoribbons with a molecular cross section is thus evaluated to be 8 or 9, based on the results from current and literature reports.

LA035505S